Magnetic Fields across the Hertzsprung-Russell Diagram
ASP Conference Series, Vol. $\pi \times 10^7$, 2001
G. Mathys, S.K. Solanki, & D.T. Wickramasinghe

Further Analysis of Stellar Magnetic Cycle Periods

Steven Saar

Harvard-Smithsonian Center for Astrophysics, 60 Garden Street, Cambridge, MA 02138, USA

Axel Brandenburg

NORDITA, Blegdamsvej 17, DK-2100 Copenhagen Ø, Denmark

Abstract. We further investigate relationships between activity cycle periods in cool stars and rotation to include new cycle data, and explore different parameterizations of the problem. We find that relations between cycle and rotational frequencies ($\omega_{\rm cyc}$ vs. Ω) and between their ratio and the inverse Rossby number ($\omega_{\rm cyc}/\Omega$ vs. ${\rm Ro}^{-1}$) show many similarities, including three branches and similar rms scatter. We briefly discuss some implications for dynamo models.

1. Introduction

Several recent studies (Ossendrijver 1998; Tobias 1998; Brandenburg et al. 1998; Saar & Brandenburg 1999 [=SB]; Lanza & Rodonò 1999) have revisited relationships between stellar magnetic cycles and other stellar properties, taking advantage of the increased quality and quality of the cycle data available (e.g., Baliunas et al. 1995). SB studied relationships between non-dimensional quantities such as cycle-to-rotational frequency ratio $\omega_{\rm cyc}/\Omega$, the normalized Ca II HK emission flux $R'_{\rm HK}$, and the inverse Rossby number ${\rm Ro}^{-1} = 2\tau_c\Omega$ (where τ_c is the convective turnover time). They found evidence for three power-law "branches" upon which stars tended to cluster. Here we expand on this work. We add new cycle data, and investigate how the new data affect various parameterizations, both dimensional and non-dimensional, of the stellar cycles, focusing on relations between $\omega_{\rm cyc}$ and rotation.

2. Data and Analysis

We combine cycle and stellar data gathered by SB with more recent measurements of plage (e.g., Hatzes et al. 2000) and spot cycles (e.g., Oláh et al. 2000). Cyclic changes in $P_{\rm rot}$ in some close binaries have been linked with magnetic cycle modulation (via changes in mean magnetic pressure) of stellar quadrupole moments (Lanza et al. 1998). These cycles based on variations in $P_{\rm rot}$ (Lanza & Rodonò 1999) are also tentatively included. We follow the strategy of SB, using theoretical τ_c (Gunn et al. 1998) and weighting the $P_{\rm cyc}$ by a "quality factor" w ($0.5 \leq w \leq 4$) depending on the strength of the periodogram signal or clarity

of the cycle modulation. We set $w = 1$ for the $P_{\rm rot}$-change cycles. Stars are assigned to branches (where appropriate) by eye to minimize fit rms. Evolved stars were not included in the fits due to less well determined τ_c. Results for different classes of stars are shown in Fig. 1 LEFT (using dimensionless $\omega_{\rm cyc}/\Omega$ and ${\rm Ro}^{-1}$) and Fig. 1 RIGHT (using $\omega_{\rm cyc} = 2\pi/P_{\rm cyc}$ and $\Omega = 2\pi/P_{\rm rot}$).

3. Results and Discussion

Our results can be summarized as follows:

(1) Three branches – denoted I (inactive), A (active), and S (super-active) – appear in both the ${\rm Ro}^{-1}$ and Ω parameterizations (Fig. 1). For the ${\rm Ro}^{-1}$ fit, the power law exponents are $\delta_I \approx -0.3$ (with a fit dispersion $\sigma_{fit} = 0.095$ dex), $\delta_A \approx -0.15$ ($\sigma_{fit} = 0.18$), and $\delta_S \approx 0.4$ ($\sigma_{fit} = 0.26$ dex); for the Ω fit, $\delta_I \approx 1.15$ ($\sigma_{fit} = 0.093$ dex), $\delta_A \approx 0.8$ ($\sigma_{fit} = 0.17$ dex), and $\delta_S \approx 0.4$ ($\sigma_{fit} = 0.24$ dex). Thus the rms scatter is similar for the two parameterizations.

(2) Secondary cycle periods ($P_{\rm rot}^{(2)}$) seen in some stars often lie on one of the branches (though this is more rare in S branch stars). The solar Gleissberg "cycle" (~ 100 years) appears to lie on the S branch. The preferred branch of the primary $P_{\rm cyc}$ (with the strongest periodogram signal) may be mass and Ω dependent. Multiple $P_{\rm cyc}$ may reflect multiple dynamo modes in an $\alpha\Omega$ framework (Knobloch, Rosner & Weiss 1981), or different dynamos existing in separate latitude zones (note the dual, separately evolving activity patterns in the double $P_{\rm cyc}$ star β Comae; Donahue & Baliunas 1992). In the Babcock-Leighton scenario, $P_{\rm rot}^{(2)}$ may be excited by stochastic variations in the poloidal source term (Charbonneau & Dikpati 2000).

(3) A single power law can be fit to the data (e.g., $\omega_{\rm cyc} \propto \Omega^{-0.09}$, SB; see also Baliunas et al. 1996) but only at the expense of a considerably higher dispersion about the fit ($\sigma_{fit} = 0.33$ dex), and loss of an explanation for the secondary cycle periods (since they no longer reside on another dynamo "branch").

(4) Evolved stars typically lie near branches, though show more scatter than the dwarfs. Since the increased scatter is seen in both parameterizations, it is unlikely to be due to less precise τ_c in evolved stars (indeed, arguably the scatter in evolved stars is reduced using ${\rm Ro}^{-1}$). The $P_{\rm cyc}$ based on $P_{\rm rot}$ variation (Lanza & Rodonò 1999) also follow the general trends. The branches are better separated using ${\rm Ro}^{-1}$. On the other hand, the Ω plot is simpler, lacking the "transitional" regime between the A and S branches seen in the ${\rm Ro}^{-1}$ diagrams. Contact binaries (gray $\diamond$; bottom panels) are poorly fit in both schemes (worse if ${\rm Ro}^{-1}$ is used); their dynamos may be altered by turbulent energy transfer toward the secondary (Hazlehurst 1985) which is independent of rotation.

(5) The branches may merge for small ${\rm Ro}^{-1}$ or Ω (though at values which might not be reached by actual stars). Curiously, the ratio of the power law exponents for the Ω fits are $\delta_I : \delta_A : \delta_S \approx 3 : 2 : 1$.

(6) Since Ω and ${\rm Ro}^{-1}$ decrease in time on the main-sequence, the relations between $\omega_{\rm cyc}$ and rotation map out dynamo evolution with time. The overlapping branches and $P_{\rm rot}^{(2)}$ suggest that $\omega_{\rm cyc}$ evolves in time in a complex, sometimes multi-valued fashion. The panels of Figure 1 LEFT show an approximate age calibration along the top axes.

A Babcock-Leighton type model predicts $\omega_{\rm cyc} \propto u_m^{0.9}$ for solar-like dwarfs (where u_m is the meridional flow velocity; Dikpati & Charbonneau 1999). If u_m increases approximately linearly with Ω in slower rotators (e.g., Brummell et al. 1998), the predicted $\omega_{\rm cyc}$ matches the I and A branches reasonably well (see also Charbonneau & Saar, this volume). Mean-field models with sufficiently strong Ω dependence for the differential rotation (e.g., Donahue et al. 1996) and the α effect (e.g., Brandenburg & Schmitt 1998) can also match the observed branches (SB; Charbonneau & Saar, this volume). We are studying a variety of dynamo models to better understand the implications of the cycle - rotation relations seen here.

Acknowledgments. This work was supported by NSF grants AST-9528563 and AST-9731652, and HST grants GO-7440 and GO-8143. We thank M. Dikpati and P. Charbonneau for enlightening discussions.

References

Baliunas, S.L., Donahue, R.A., Soon, W. et al. 1995, ApJ 438, 269

Baliunas, S.L., Nesme-Ribes, E., Sokoloff, D., & Soon, W. 1996, ApJ 460, 848

Brandenburg, A., Saar, S.H., & Turpin, C.J. 1998, ApJ 498, L51

Brandenburg, A., & Schmitt, D. 1998, A&A 338, L55

Brummell, N.H., Hurlburt, N.E., & Toomre, J. 1998, ApJ 493, 955

Charbonneau, P. & Dikpati, M. 2000, ApJ 543, 1027

Dikpati, M. & Charbonneau, P. 1999, ApJ 518, 508

Donahue, R.A. & Baliunas, S.L. 1992, ApJ 393, L63

Donahue, R.A., Saar, S.H., & Baliunas, S.L. 1996, ApJ 466, 384

Gunn, A.G., Mitrou, C.K., & Doyle, J.G. 1998, MNRAS 296, 150

Hatzes, A.P., Cochran, W.D., McArthur, B. et al. 2000, ApJ 544, 145

Hazlehurst, J. 1985, A&A 145, 25

Knobloch, E., Rosner, R., & Weiss, N.O. 1981, MNRAS 197, 45

Lanza, A., & Rodonò, M. 1999, A&A 349, 887

Lanza, A., et al. 1998, MNRAS 296, 893

Oláh, K., Kolláth, Z., & Strassmeier, K.G. 2000, A&A 356, 643

Ossendrijver, A.J.H. 1997, A&A 323, 151

Saar, S.H., & Brandenburg, A. 1999, ApJ 524, 295 [=SB]

Tobias, S.M. 1998, MNRAS 296, 653

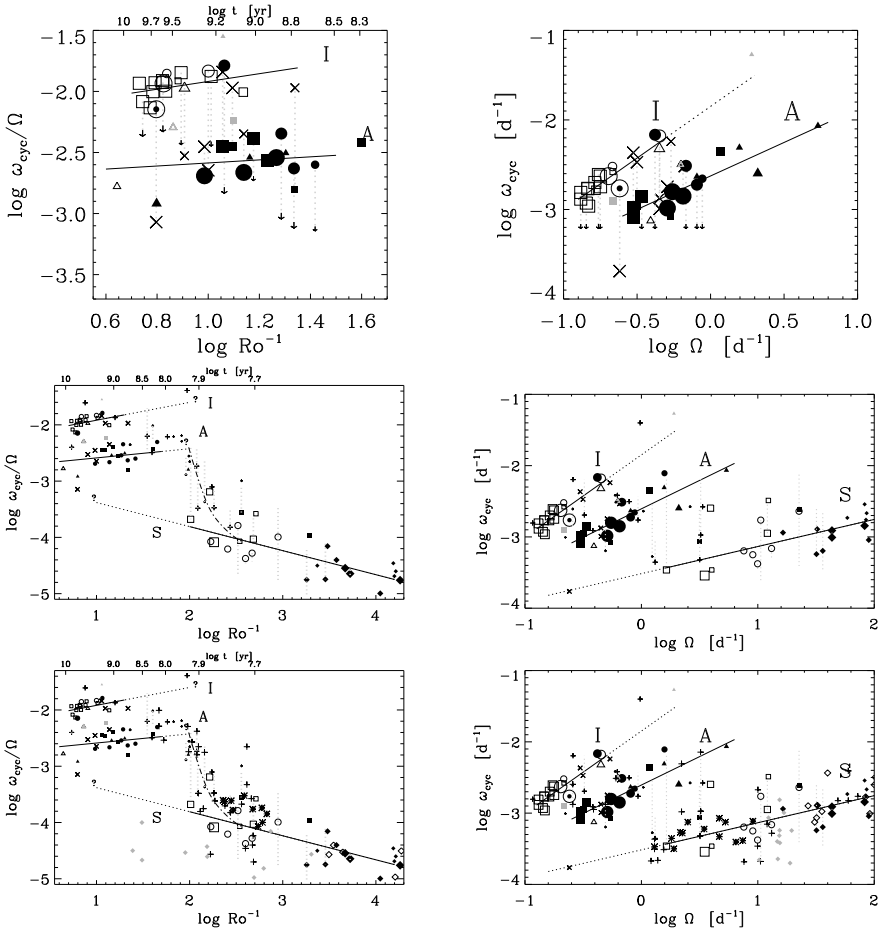

Figure 1. LEFT top: $\omega_{\rm cyc}/\Omega$ vs. Ro^{-1} for single dwarfs; symbols indicate the sun ($\odot$), F ($\triangle$), G ($\circ$), and K ($\square$) stars (filled if $\log R'_{\rm HK} \geq -4.75$; size $\propto \sqrt{w}$, the $P_{\rm cyc}$ "reliability"). Dotted vertical lines connect two $P_{\rm cyc}$ (a $\times$ marks $P^{(2)}_{\rm rot}$), or $P_{\rm cyc}$ with a long-term trend (i.e., a possible $P^{(2)}_{\rm rot} > 25$ yr; arrow symbol). Weighted least square fits ($\omega_{\rm cyc}/\Omega \propto \mathrm{Ro}^{\delta}$) for the active (A) and inactive (I) branches are shown (solid); $\delta_I = -0.32$ and $\delta_A = -0.16$. LEFT middle: same, including binaries (BY Dra, CV secondaries; M stars = $\diamond$) and RS CVns (+; not included in the fits). A "superactive" (S) branch appears, with $\delta_S = +0.43$ ($P^{(2)}_{\rm rot} \leftrightarrow P_{\rm cyc}$ lines shown only for new stars). A transitional regime between the A and S branches is indicated (dash-dot). LEFT bottom: same, including cycles based on $P_{\rm rot}$ variation in RS CVns (new +), CV secondaries (open $\diamond$), Algols ($*$), and contact binaries (gray $\diamond$). RIGHT top: $\omega_{\rm cyc}$ vs. Ω for single dwarfs. Fits ($\omega_{\rm cyc} \propto \Omega^{\delta}$) for the A and I branches (solid) yield $\delta_I = 1.15$ and $\delta_A = 0.80$. RIGHT middle: same, including binaries (like LEFT middle). The new S branch shows $\delta_S = 0.38$. RIGHT bottom: same, including $P_{\rm rot}$ variation cycles (like LEFT bottom).